

# Resonant Acoustic Mixing (RAM) for Efficient Mechano-redox Catalysis without Grinding or Impact Media

Farshid Effaty,<sup>a,b</sup> Lori Gonnet,<sup>b</sup> Stefan G. Koenig,<sup>c</sup> Karthik Nagapudi,<sup>c</sup> Xavier Ottenwaelder,<sup>\*a</sup> and Tomislav Friščić<sup>\*b,d</sup>

<sup>a</sup> Department of Chemistry and Biochemistry, Concordia University, 7141 Sherbrooke St. W., Montreal, QC, H4B 1R6, Canada

<sup>b</sup> Department of Chemistry, McGill University, 801 Sherbrooke St. West, Montreal, QC, H3H 0B8, Canada

<sup>c</sup> Small molecule Pharmaceutical Sciences, Genentech Inc., One DNA Way, South San Francisco, CA 94080, USA

<sup>d</sup> School of Chemistry, University of Birmingham, Edgbaston, Birmingham, B15 2TT, United Kingdom

## Table of Contents

<b>1. Materials and methods</b>	<b>2</b>
1.1. Materials and chemicals	2
1.2. Resonant acoustic mixing (RAM)	2
1.3. Solution NMR spectroscopy	2
1.4. Solid-state NMR spectroscopy	2
1.5. High-resolution mass spectrometry	2
1.6. FTIR-ATR spectroscopy	2
1.7. Scanning Electron Microscopy	2
1.8. X-ray Photoelectron Spectroscopy (XPS)	2
1.9. Powder X-ray diffraction (PXRD)	2
1.10. Single-Crystal X-ray diffractions	2
<b>2. General procedure of making aryldiazonium tetrafluoroborate salts</b>	<b>2</b>
<b>3. General procedure for the RAM synthesis of compounds 2a-2j</b>	<b>3</b>
<b>4. Crystallographic data for compound TEMPO-trapped intermediate</b>	<b>3</b>
<b>5. FTIR-ATR Analysis of Barium Titanate Before and After Calcination.</b>	<b>3</b>
<b>6. FTIR-ATR and PXRD of Recycled BaTiO<sub>3</sub> from Ball-milling Experiments.</b>	<b>4</b>
<b>7. X-ray Photoelectron Spectroscopy (XPS) Analysis of Recycled Barium Titanate</b>	<b>5</b>
<b>8. Solid-state NMR Spectroscopy of Pristine and Recycled Barium Titanate</b>	<b>6</b>
<b>9. Effect of the Amount of Barium Titanate</b>	<b>6</b>
<b>10. Summary of <sup>1</sup>H and <sup>13</sup>C NMR and HR-MS Data</b>	<b>7</b>
<b>11. FTIR-ATR Spectra for Isolated Products 2a-2j</b>	<b>10</b>
<b>12. <sup>1</sup>H and <sup>13</sup>C NMR Data for Isolated Products 2a-2j and TEMPO-trapped intermediate</b>	<b>14</b>
<b>13. References</b>	<b>26</b>

## 1. Materials and methods

### 1.1. Materials and chemicals

Unless otherwise specified, all reagents and solvents were obtained from commercial sources and used without further purification. Cubic barium titanate was obtained from Sigma-Aldrich as nanopowder, <100 nm particle size (BET),  $\geq 99\%$  trace metals basis, and was used as is.

### 1.2. Resonant acoustic mixing (RAM)

Synthesis of all compounds were carried out in a LabRAM II (Resodyn) using 2.5 mL polypropylene vials. A RAM sample holder made of Delrex plastic was developed (Figure 1 in manuscript) to ensure reproducibility and perform multiple experiments simultaneously.

### 1.3. Solution NMR spectroscopy

$^1\text{H}$  NMR,  $^{13}\text{C}$  NMR and  $^{19}\text{F}$  NMR spectra were recorded on a Bruker AVIIIHD 500MHz NMR spectrometer. Chemical shifts are reported relative to DMSO- $d_6$  ( $\delta$  2.50) or  $\text{CDCl}_3$  ( $\delta$  7.26) and data is presented as chemical shifts, and integration.

### 1.4. Solid-state NMR spectroscopy

The  $^{11}\text{B}$  MAS spectra was acquired on a Varian VNMRS (now Agilent, Santa Clara, CA, USA) spectrometer operating at 399.8 MHz for  $^1\text{H}$  and 128.6 MHz for  $^{11}\text{B}$  using a 4 mm double-resonance Varian Chemagnetics T3 probe (now Agilent, Santa Clara, CA, USA). Approximately 30 mg of sample were center-packed into rotors using Kel-F inserts and spun at 15 kHz. The spectra were acquired in 256 scans using a recycle delay of 2 s. SPINAL-64 decoupling at a rf field of 90 kHz was applied during acquisition. NMR yields are based on  $^1\text{H}$  NMR analysis of the reaction mixture after dissolution in DMSO- $d_6$ .

### 1.5. High-resolution mass spectrometry

The  $m/z$  ratios of the purified products were obtained on high-resolution mass spectrometers using ESI or ACPI ionization methods.

### 1.6. FTIR-ATR spectroscopy

Infrared spectra were obtained using a Bruker Platinum attenuated total reflectance (ATR) spectrometer and are reported in wavenumber ( $\text{cm}^{-1}$ ) units.

### 1.7. Scanning Electron Microscopy

SEM data was collected on a Phenom ProX SEM Scanning Electron Microscope with EDS. Samples were loaded on carbon tape by dispersion in air and analyzed without coatings to minimize surface modifications.

### 1.8. X-ray Photoelectron Spectroscopy (XPS)

X-ray photoelectron spectroscopy (XPS) was conducted on a Fischer Scientific  $\text{K}\alpha$  X-ray spectrometer with an excitation source of  $\text{Al K}\alpha = 1486.6$  eV. A spot size of 400  $\mu\text{m}$  was used, running 5 survey scans at 200 mV for 50 ms residence times, and 10 scans for specific elements, also at residence times of 50 ms. Deconvolution and peak position were determined using Avantage processing software.

### 1.9. Powder X-ray diffraction (PXRD)

PXRD patterns were obtained in the  $2\theta$  range from  $4^\circ$  to  $60^\circ$  using a Bruker D2 PHASER X-Ray Diffractometer equipped with a  $\text{Cu-K}\alpha$  ( $\lambda = 1.54 \text{ \AA}$ ) source, LinxEye detector, and a Ni filter.

### 1.10. Single-Crystal X-ray diffractions

Crystallography experiments were conducted on a Bruker D8 Venture with a PHOTON-II detector at the  $\text{Cu-K}\alpha$  ( $\lambda = 1.54 \text{ \AA}$ ) radiation. Solution and refinement were performed with APEX and OLEX2 software.

## 2. General procedure of making aryldiazonium tetrafluoroborate salts

Known aryldiazonium tetrafluoroborates (**1a–1i**) were made from the respective anilines.<sup>1</sup> Aniline (10.0 mmol) was added to 4 mL of distilled water and 3.5 mL of fluoroboric acid complexed by ether ( $\text{HBF}_4 \cdot \text{Et}_2\text{O}$ ) and the mixture was cooled down to  $0^\circ\text{C}$  using an ice-bath. An aqueous potassium nitrite ( $\text{KNO}_2$ ) solution (700 mg, 10.1 mmol, in 1.5 mL  $\text{H}_2\text{O}$ ) was added dropwise over 5 minutes while stirring. For the bis(diazonium) substrate **2j**, these quantities were doubled with respect to the aromatic amine. After 30 minutes of stirring under ice-bath conditions, the thick precipitate was collected by filtration and redissolved in the minimum amount of acetone. Diethyl ether was added until the aryldiazonium tetrafluoroborate precipitated, after which it was filtered, repeatedly washed with diethyl ether, and dried under vacuum. *Safety measures are recommended while working with aryldiazonium salts, although throughout this research no accident had occurred.*<sup>2</sup>

The large-scale synthesis of the extensively used *p*-chlorophenyldiazonium tetrafluoroborate (up to 20 grams) was performed with using extra safety measures such as using a safety shield inside the fumehood. For scale-up synthesis, the reagents were scaled up with respect to the amount of aniline used by the same ratio.

### 3. General procedure for the RAM synthesis of compounds 2a-2j

In a typical experiment, the aryldiazonium tetrafluoroborate salt (0.3 mmol, 1 eq), bis(pinacolato)boron (0.3 mmol, 1 eq) and barium titanate (4.3 equivalents, 1.29 mmol) were added to a 2.5 mL polypropylene vial. Acetonitrile ( $\eta = 0.25$   $\mu\text{L}/\text{mg}$ ) was added to the vial and the mixture mixed using the LabRAM II instrument between 1 and 3 hours, at 90g acceleration. The conversion was evaluated by  $^1\text{H}$  NMR analysis of a solution obtained by dissolving the entire crude reaction mixture in DMSO- $d_6$ . The pinacol ester phenyls **2a-2j** were purified by silica gel column chromatography using hexanes/EtOAc (100:00 to 90:10) as eluent unless specified otherwise. The resulting product was dried under reduced pressure and characterized by  $^1\text{H}$ -NMR,  $^{13}\text{C}$ -NMR, FTIR-ATR and Mass Spectrometry.

### 4. Crystallographic data for compound TEMPO-trapped intermediate

**Table S1.** Crystallographic data for TEMPO-trapped intermediate.

	(CCDC deposition No.: 2205247)
Molecular formula	$\text{C}_{15}\text{H}_{22}\text{N}_2\text{O}_3$
$M_r$	278.34
Crystal system	Monoclinic
Crystal colour	Yellow
Space group	Cc
Temperature (K)	298.15
Unit cell dimensions ( $\text{\AA}$ , $^\circ$ )	
$a$	17.1295(4)
$b$	17.2313(4)
$c$	42.1825(11)
$\alpha$	90
$\beta$	92.099(2)
$\gamma$	90
Volume ( $\text{\AA}^3$ )	12442.4(5)
$Z$	32
$r_{\text{calc}}$ ( $\text{g cm}^{-3}$ )	1.189
$\mu$ ( $\text{mm}^{-1}$ )	0.674
$F(000)$	4800.0
Refl. Collected/independent	119759 / 24094
No. observed refl. [ $I > 2s(I)$ ]*	17385
No. restraints/No. parameters	2/ 1475
$R/wR$ [all data]	0.0981 / 0.2434
Goodness-of-fit on $F^2$	1.067

\* $R = \frac{\sum ||F_o| - |F_c||}{\sum F_o}$ ,  $w = 1/[\sigma^2(F_o^2) + (g_1P)^2 + g_2P]$  where  $P = (F_o^2 + 2F_c^2)/3$ ,  $S = \frac{\sum [w(F_o^2 - F_c^2)]^2}{(N_{\text{obs}} - N_{\text{param}})}$ <sup>1/2</sup>.

### 5. FTIR-ATR Analysis of Barium Titanate Before and After Calcination.

Barium titanate in its pristine form was heated under continuous flow of  $\text{N}_2$  at 800  $^\circ\text{C}$  for 12 hours using a Mettler Toledo Thermogravimetric Analyzer (TGA) instrument and the resulting material was analyzed by FTIR-ATR in order to detect the loss of carbonate component.

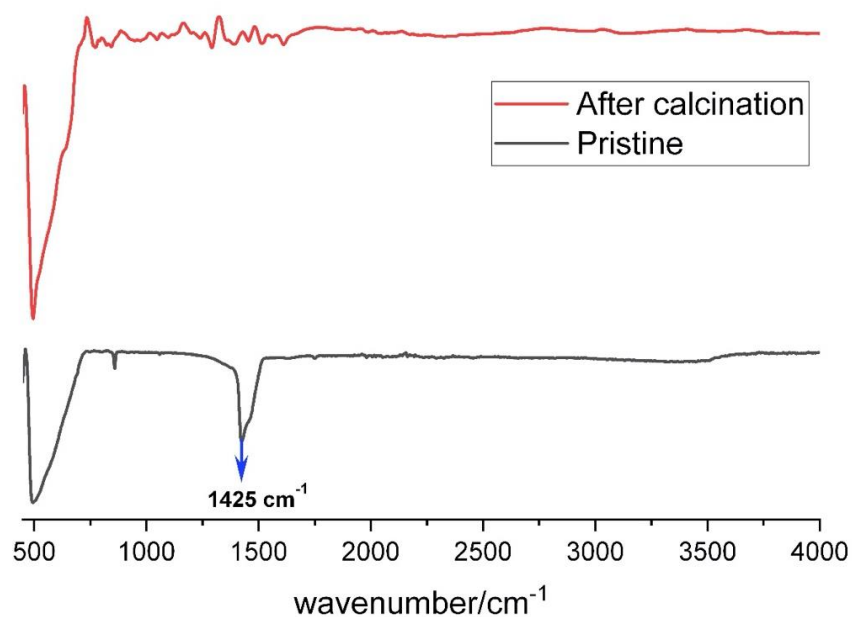


**Figure S1.** FTIR-ATR spectra of barium titanate before (bottom) and after (top) treatment at 800 °C under N<sub>2</sub>.

## 6. FTIR-ATR and PXRD of Recycled BaTiO<sub>3</sub> from Ball-milling Experiments.

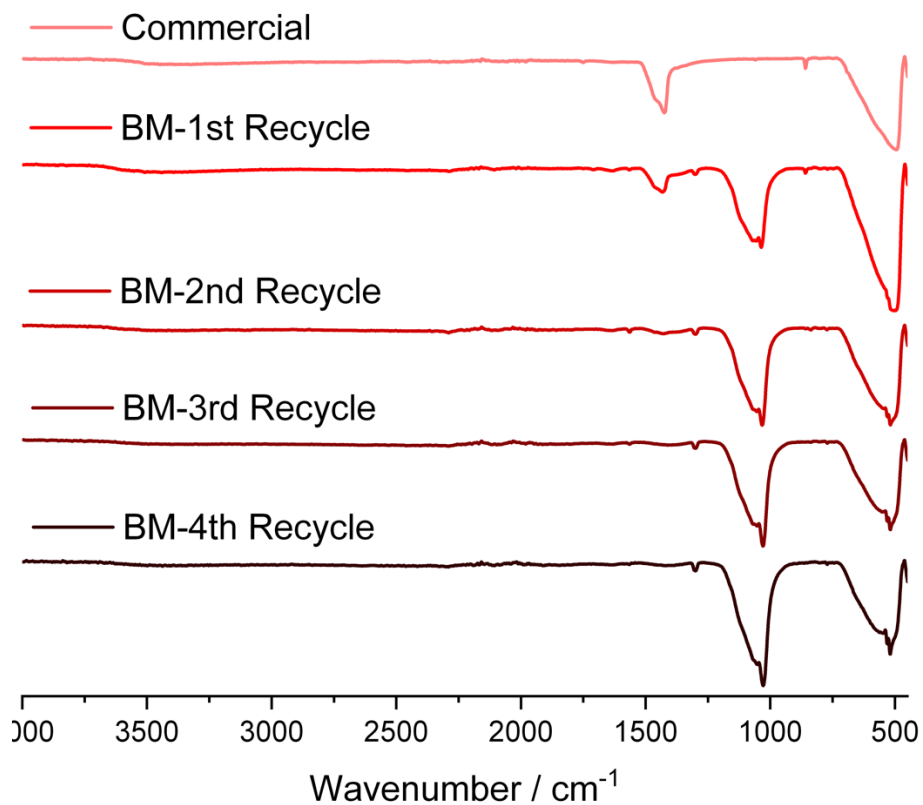


**Figure S2.** Comparison of FTIR-ATR spectra of BaTiO<sub>3</sub> after recycling from consecutive ball-milling reactions.

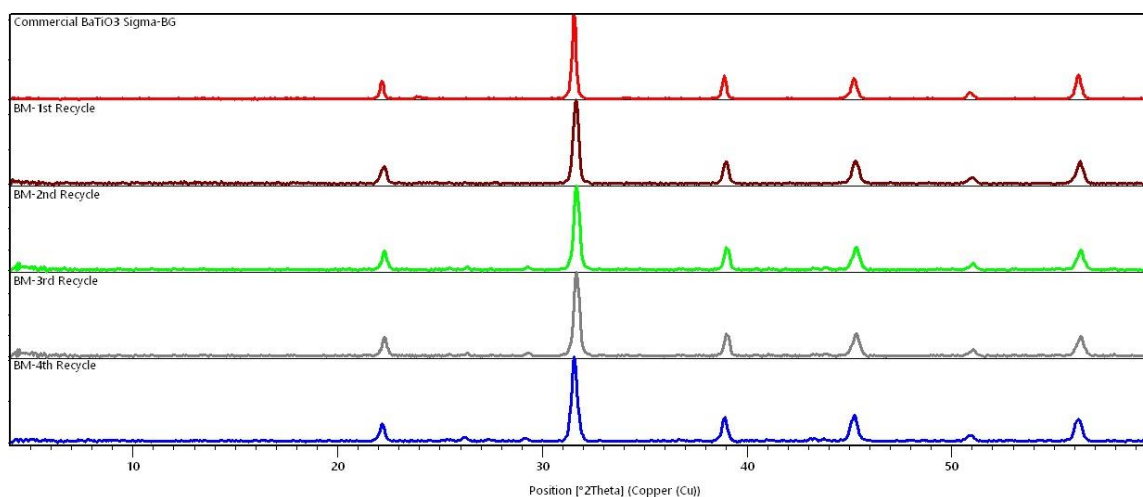


**Figure S3.** Comparison of PXRD patterns for BaTiO<sub>3</sub> after recycling from consecutive ball-milling mechanoredox borylation reactions involving **1a** and **bpb**.

## 7. X-ray Photoelectron Spectroscopy (XPS) Analysis of Recycled Barium Titanate

Recycled barium titanate from the mechanoredox borylation by RAM has been washed with EtOAc and dried under high vacuum and then analyzed by X-ray photoelectron spectroscopy (XPS).

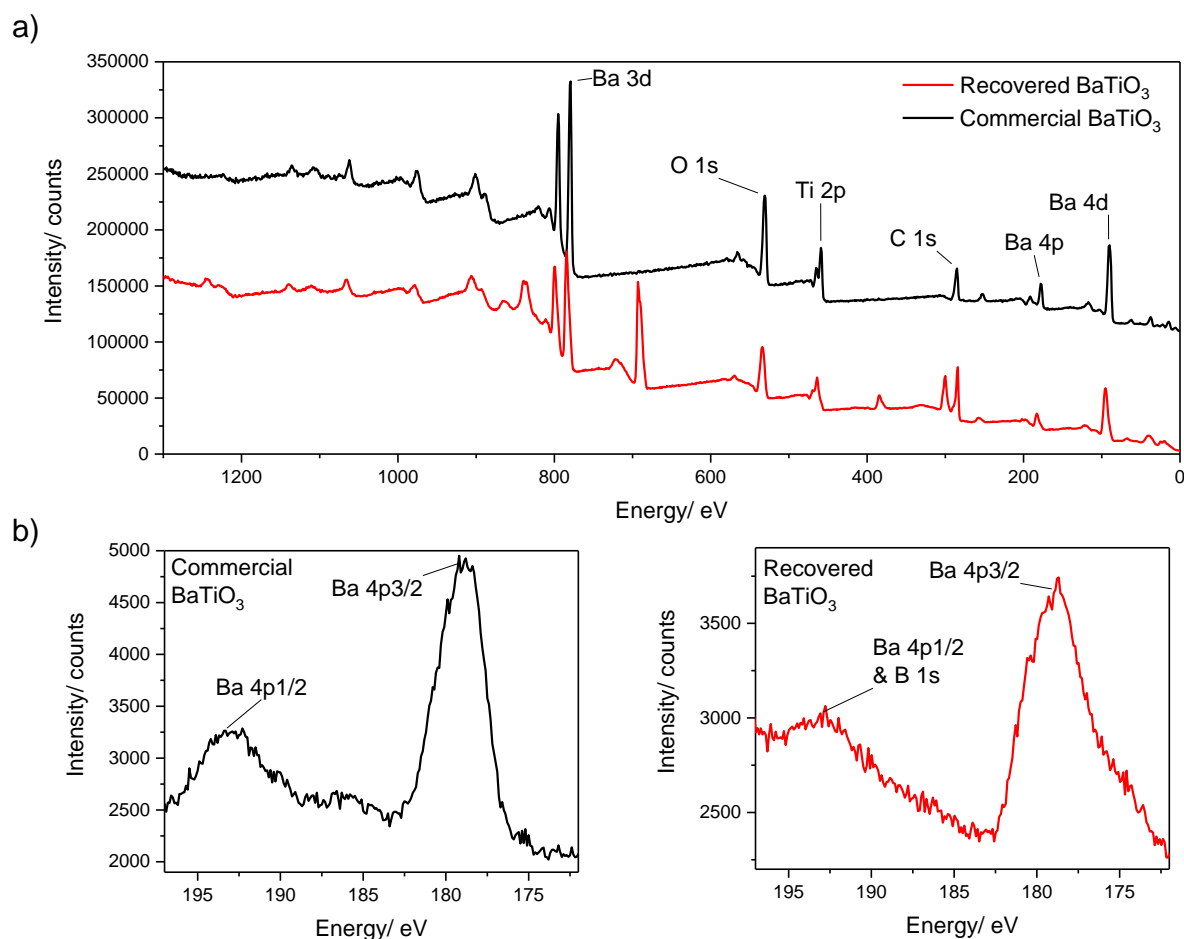


**Figure S4.** a) XPS surveys of the pristine and recovered BaTiO<sub>3</sub> b) B 1s region scan of the pristine and recovered BaTiO<sub>3</sub>.

## 8. Solid-state NMR Spectroscopy of Pristine and Recycled Barium Titanate

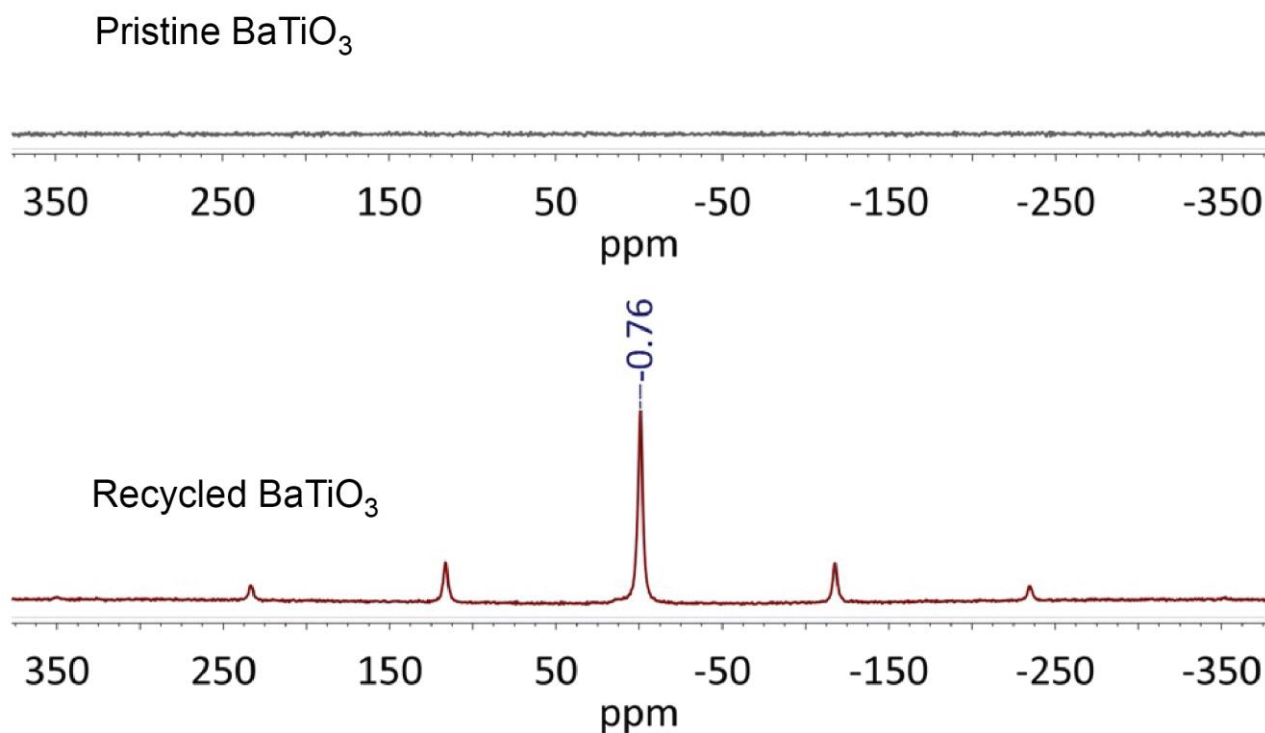


**Figure S5.** Comparison of the <sup>11</sup>B ssNMR spectra for (top) pristine BaTiO<sub>3</sub> and (bottom) BaTiO<sub>3</sub> recycled from a RAM mechanoredox reaction.

## 9. Effect of the Amount of Barium Titanate

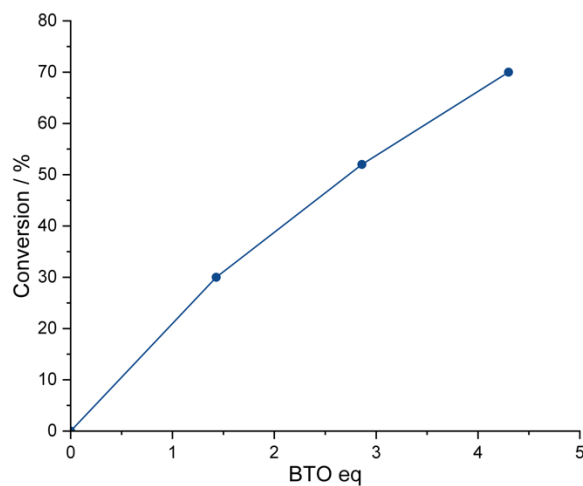
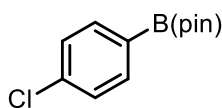


**Figure S6.** Effect of the amount of barium titanate on reaction conversion of *p*-chlorophenyldiazonium tetrafluoroborate (**1a**) with bis(pinacolato)diboron (**bpb**) after 1 hour RAM in presence of MeCN at 90g.

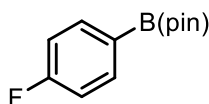
## 10. Summary of $^1\text{H}$ and $^{13}\text{C}$ NMR and HR-MS Data

### 2-(4-chlorophenyl)-4,4,5,5-tetramethyl-1,3,2-dioxaborolane 2a



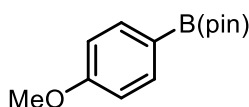
$^1\text{H}$  NMR (500 MHz, DMSO)  $\delta$  7.67 (d,  $J$  = 10.0 Hz, 2H), 7.45 (d,  $J$  = 10 Hz, 2H), 1.29 (s, 12H).  $^{13}\text{C}$  NMR (126 MHz, DMSO)  $\delta$  136.95, 136.65, 128.51, 84.40, 25.12. Because of quadrupolar relaxation, the carbon directly attached to the boron atom was not detected.<sup>3,4</sup> HRMS APCI (+): calculated for  $\text{C}_{12}\text{H}_{17}\text{BClO}_2$ , 239.1010; found, 239.1005.

### 2-(4-fluorophenyl)-4,4,5,5-tetramethyl-1,3,2-dioxaborolane 2b



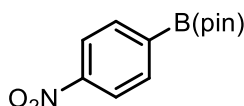
$^1\text{H}$  NMR (500 MHz, DMSO)  $\delta$  7.72 (t,  $J$  = 10.0 Hz, 2H), 7.21 (t,  $J$  = 10 Hz, 2H), 1.30 (s, 12H).  $^{13}\text{C}$  NMR (126 MHz, DMSO)  $\delta$  165.88, 137.42 (d,  $J_{\text{C-F}}$  = 8.8 Hz), 115.49 (d,  $J_{\text{C-F}}$  = 20.2 Hz), 84.29, 25.13.  $^{19}\text{F}$  NMR (471 MHz,  $\text{CDCl}_3$ )  $\delta$  -108.46. Because of quadrupolar relaxation, the carbon directly attached to the boron atom was not detected.<sup>3,4</sup>

### 2-(4-methoxyphenyl)-4,4,5,5-tetramethyl-1,3,2-dioxaborolane 2c



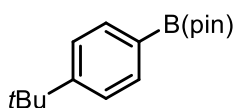
$^1\text{H}$  NMR (500 MHz,  $\text{CDCl}_3$ )  $\delta$  7.75 (d,  $J$  = 10 Hz, 2H), 6.90 (d,  $J$  = 10, 2H), 3.83 (s, 3H), 1.33 (s, 12H).  $^{13}\text{C}$  NMR (126 MHz,  $\text{CDCl}_3$ )  $\delta$  162.16, 136.52, 113.32, 83.56, 55.10, 24.87. Because of quadrupolar relaxation, the carbon directly attached to the boron atom was not detected.<sup>3,4</sup> HRMS APCI (+): calculated for  $\text{C}_{13}\text{H}_{20}\text{BO}_3$ , 235.1505; found, 235.1500.

### 4,4,5,5-tetramethyl-2-(4-nitrophenyl)-1,3,2-dioxaborolane 2d



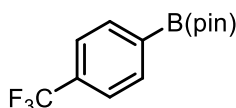
$^1\text{H}$  NMR (500 MHz,  $\text{CDCl}_3$ )  $\delta$  8.19 (d,  $J$  = 10 Hz, 2H), 7.96 (d,  $J$  = 10 Hz, 2H), 1.37 (s, 12H).  $^{13}\text{C}$  NMR (126 MHz,  $\text{CDCl}_3$ )  $\delta$  149.87, 135.67, 122.43, 84.64, 24.89. Because of quadrupolar relaxation, the carbon directly attached to the boron atom was not detected.<sup>3,4</sup> HRMS APCI (+): calculated for  $\text{C}_{12}\text{H}_{17}\text{BNO}_4$ , 250.1251; found, 250.1245.

### 2-(4-(tert-butyl)phenyl)-4,4,5,5-tetramethyl-1,3,2-dioxaborolane 2e



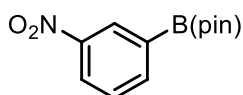
$^1\text{H}$  NMR (500 MHz,  $\text{CDCl}_3$ )  $\delta$  7.76 (d,  $J$  = 10 Hz, 2H), 7.41 (d,  $J$  = 10 Hz, 2H), 1.33 (s, 12H), 1.32 (s, 9H).  $^{13}\text{C}$  NMR (126 MHz,  $\text{CDCl}_3$ )  $\delta$  154.51, 134.70, 124.71, 83.62, 34.90, 31.21, 24.85. Because of quadrupolar relaxation, the carbon directly attached to the boron atom was not detected.<sup>3,4</sup> HRMS APCI (+): calculated for  $\text{C}_{16}\text{H}_{26}\text{BO}_2$ , 261.2026; found, 261.2020.

### 4,4,5,5-tetramethyl-2-(4-(trifluoromethyl)phenyl)-1,3,2-dioxaborolane 2f



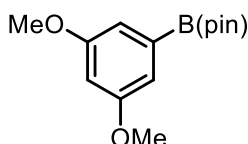
$^1\text{H}$  NMR (500 MHz,  $\text{CDCl}_3$ )  $\delta$  7.91 (d,  $J$  = 7.5 Hz, 2H), 7.61 (d,  $J$  = 7.5 Hz, 2H), 1.36 (s, 12H).  $^{13}\text{C}$  NMR (126 MHz,  $\text{CDCl}_3$ )  $\delta$  135.04, 132.13, 124.35, 124.20, 84.32, 24.92. Because of quadrupolar relaxation, the carbon directly attached to the boron atom was not detected.<sup>3,4</sup>

**4,4,5,5-tetramethyl-2-(3-nitrophenyl)-1,3,2-dioxaborolane 2g**



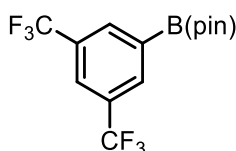
$^1\text{H}$  NMR (500 MHz,  $\text{CDCl}_3$ )  $\delta$  8.64 (s, 1H), 8.29 (d,  $J = 9.2$  Hz, 1H), 8.10 (d,  $J = 9.2$  Hz, 1H), 7.54 (t,  $J = 7.9$  Hz, 1H) 1.37 (s, 12H).  $^{13}\text{C}$  NMR (126 MHz,  $\text{CDCl}_3$ )  $\delta$  147.86, 140.65, 129.43, 128.75, 125.88, 84.61, 25.03. Because of quadrupolar relaxation, the carbon directly attached to the boron atom was not detected.<sup>3,4</sup> HRMS APCI (+): calculated for  $\text{C}_{12}\text{H}_{17}\text{BNO}_4$ , 250.1251; found, 250.1258.

**2-(3,5-dimethoxyphenyl)-4,4,5,5-tetramethyl-1,3,2-dioxaborolane 2h**



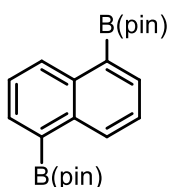
$^1\text{H}$  NMR (500 MHz,  $\text{CDCl}_3$ )  $\delta$  6.95 (d,  $J = 2$  Hz, 2H), 6.56 (t,  $J = 2.5$  Hz, 1H), 3.81 (s, 6H), 1.34 (s, 12H).  $^{13}\text{C}$  NMR (126 MHz,  $\text{CDCl}_3$ )  $\delta$  160.44, 111.65, 104.57, 83.92, 55.46, 24.89. Because of quadrupolar relaxation, the carbon directly attached to the boron atom was not detected.<sup>3,4</sup>

**2-(3,5-bis(trifluoromethyl)phenyl)-4,4,5,5-tetramethyl-1,3,2-dioxaborolane 2i**



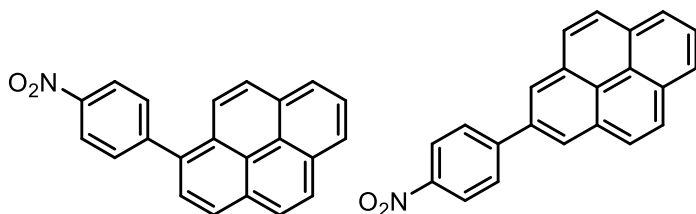
$^1\text{H}$  NMR (500 MHz,  $\text{CDCl}_3$ )  $\delta$  8.23 (s, 2H), 7.94 (s, 1H) 1.37 (s, 12H).  $^{13}\text{C}$  NMR (126 MHz, DMSO)  $\delta$  134.69, 130.93 (d,  $J_{\text{C-F}} = 36.79$ ), 124.80-124.62 (m), 122.45, 84.89, 24.91.  $^{19}\text{F}$  NMR (471 MHz,  $\text{CDCl}_3$ )  $\delta$  -62.84 (s). Because of quadrupolar relaxation, the carbon directly attached to the boron atom was not detected.<sup>3,4</sup>

**1,5-bis(4,4,5,5-tetramethyl-1,3,2-dioxaborolan-2-yl)naphthalene 2j**



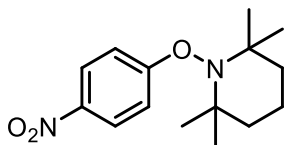
$^1\text{H}$  NMR (500 MHz,  $\text{CDCl}_3$ )  $\delta$  8.88 (d,  $J = 8.5$  Hz, 2H), 8.06 (d,  $J = 7.5$  Hz, 2H), 7.51 (t,  $J = 8$  Hz, 2H), 1.42 (s, 24H).  $^{13}\text{C}$  NMR (126 MHz,  $\text{CDCl}_3$ )  $\delta$  136.73, 135.31, 131.97, 125.42, 83.70, 24.98. Because of quadrupolar relaxation, the carbon directly attached to the boron atom was not detected.<sup>3,4</sup> HRMS APCI (+): calculated for  $\text{C}_{22}\text{H}_{30}\text{B}_2\text{O}_4$ , 381.2408; found, 381.2375.

**1-(4-nitrophenyl)pyrene 3a and 2-(4-nitrophenyl)pyrene 3b**



**3a:**  $^1\text{H}$  NMR (500 MHz,  $\text{CDCl}_3$ )  $\delta$  8.43 (dt,  $J = 8.5$  Hz, 2H), 8.27-8.24 (m, 2H), 8.22 (d,  $J = 7.5$  Hz, 1H), 8.17-8.03 (m, 5H), 7.96 (d,  $J = 7.5$  Hz, 1H), 7.81 (d,  $J = 7.5$  Hz, 2H).  $^{13}\text{C}$  NMR (126 MHz,  $\text{CDCl}_3$ )  $\delta$  148.10, 147.06, 134.82, 131.39, 131.35, 130.92, 130.72, 128.31, 128.23, 128.13, 127.22, 127.10, 126.27, 125.65, 125.28, 124.86, 124.67, 124.64, 124.11, 123.61. HRMS APCI (+): calculated for  $\text{C}_{22}\text{H}_{14}\text{NO}_2$ , 324.1024; found, 324.1019.

**2,2,6,6-tetramethyl-1-(4-nitrophenoxy)piperidine TEMPO-trapped intermediate**



$^1\text{H NMR}$  (300 MHz,  $\text{CDCl}_3$ )  $\delta$  8.14 (d,  $J = 9.2$  Hz, 2H), 7.26 (br, 2H), 1.66-1.56 (m, 5H), 1.47-1.40 (m, 1H), 1.24 (s, 6H), 0.99 (s, 6H).  $^{13}\text{C NMR}$  (75 MHz,  $\text{CDCl}_3$ )  $\delta$  168.64, 142.19, 125.53, 114.13, 60.88, 39.65, 32.25, 20.44, 16.85. HRMS ESI (+): HRMS APCI (+): calculated for  $\text{C}_{15}\text{H}_{23}\text{N}_2\text{O}_3$ , 279.1709; found, 279.1703.

## 11. FTIR-ATR Spectra for Isolated Products 2a-2j

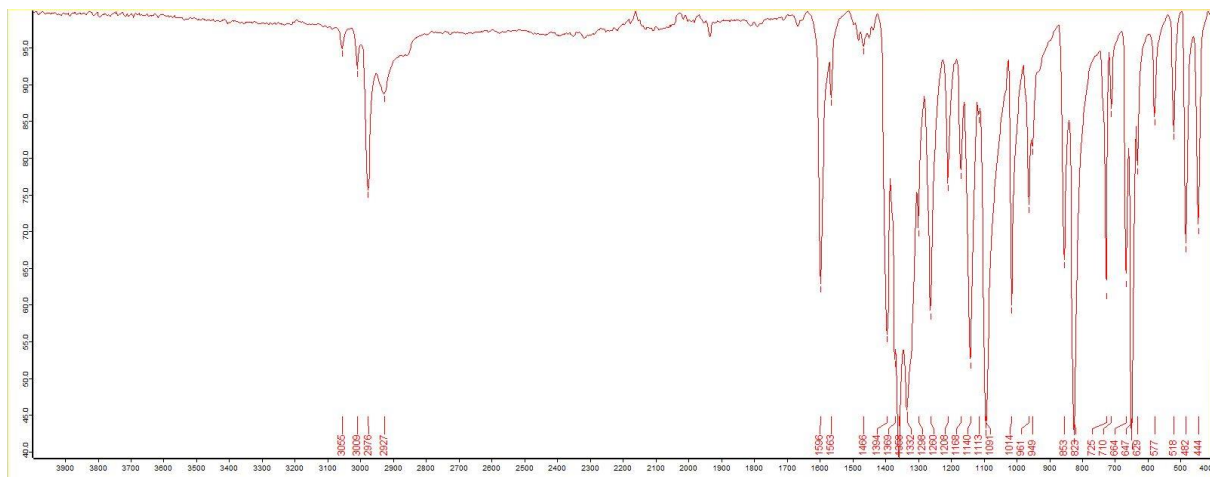


**Figure S7.** FTIR-ATR spectrum of isolated compound **2a**, synthesized by RAM.

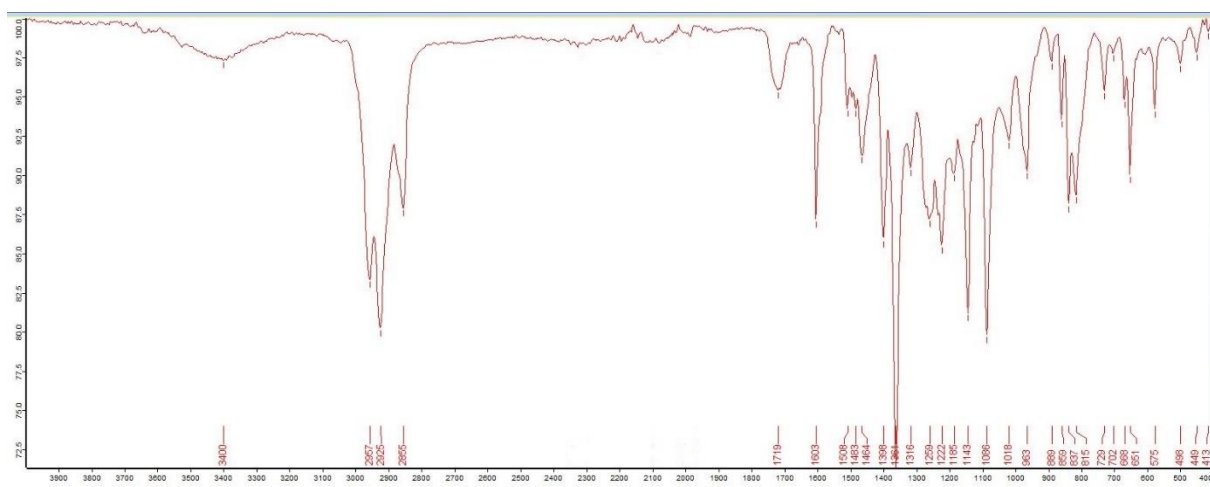


**Figure S8.** FTIR-ATR spectrum of isolated compound **2b**, synthesized by RAM.

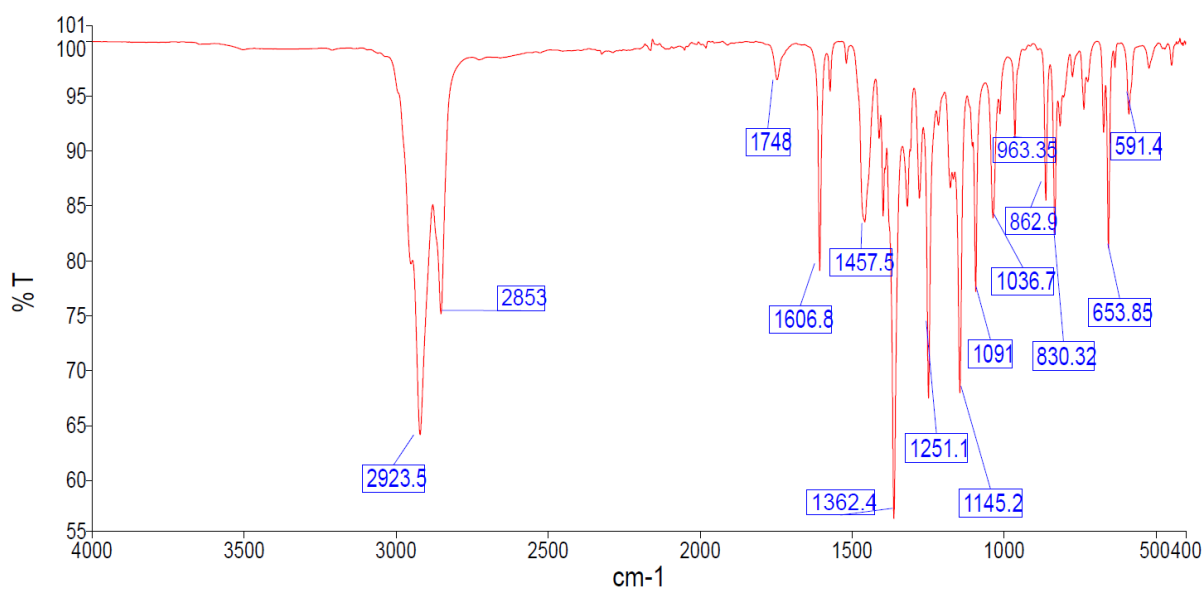


**Figure S9.** FTIR-ATR spectrum of isolated compound **2c**, synthesized by RAM.

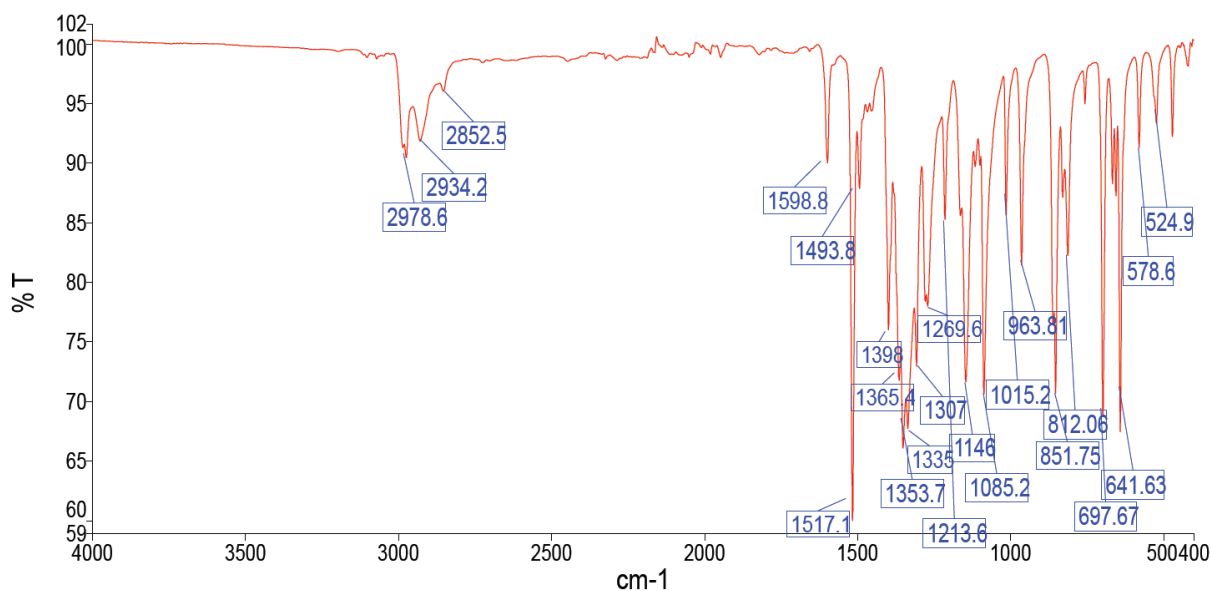


**Figure S10.** FTIR-ATR spectrum of isolated compound **2d**, synthesized by RAM.

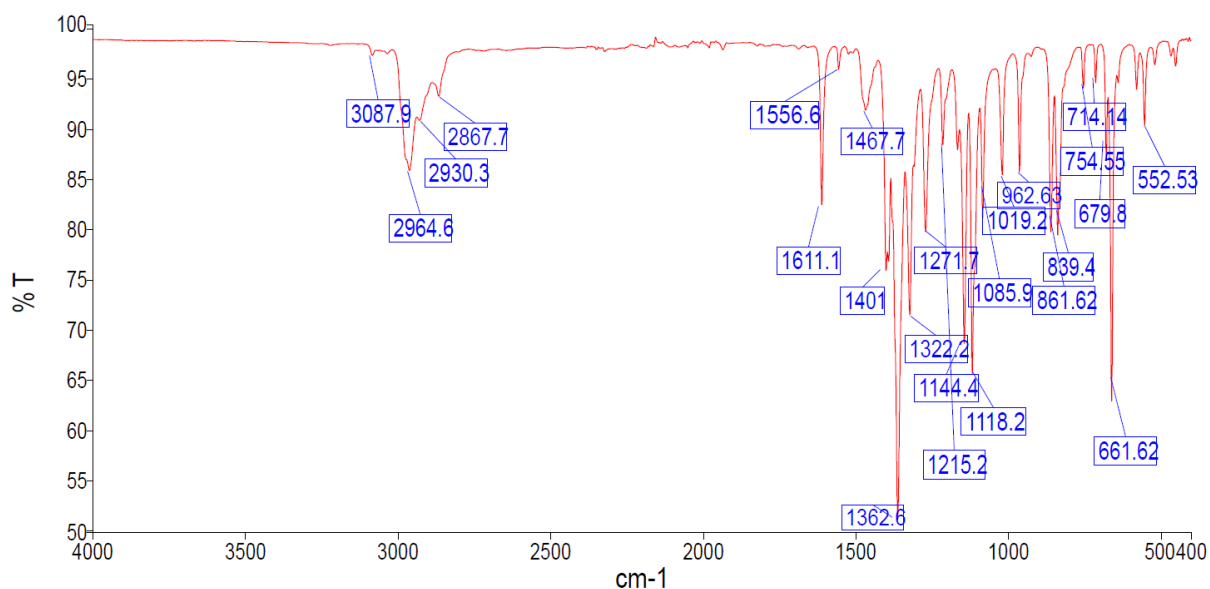


**Figure S11.** FTIR-ATR spectrum of isolated compound **2e**, synthesized by RAM.

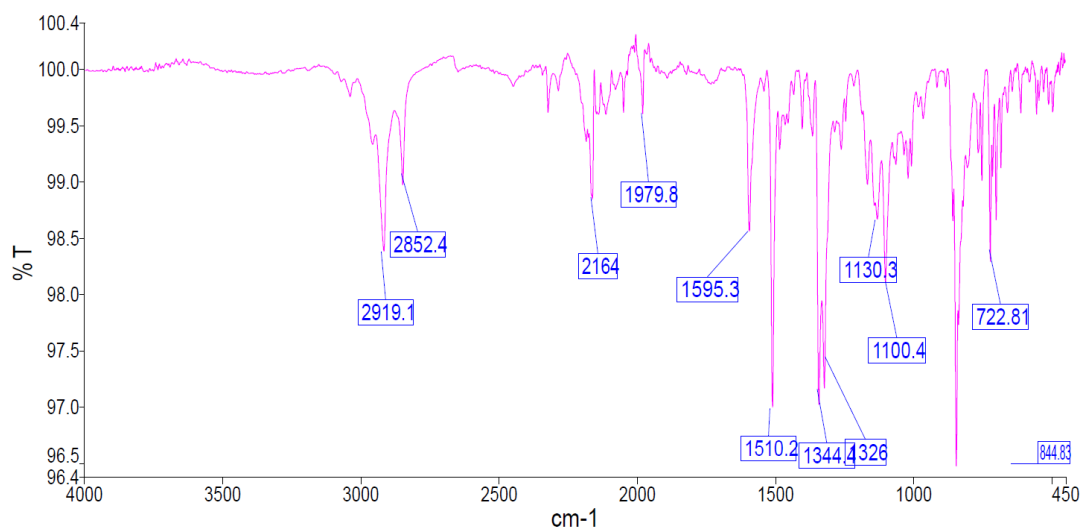


**Figure S12.** FTIR-ATR spectrum of isolated compound **2f**, synthesized by RAM.

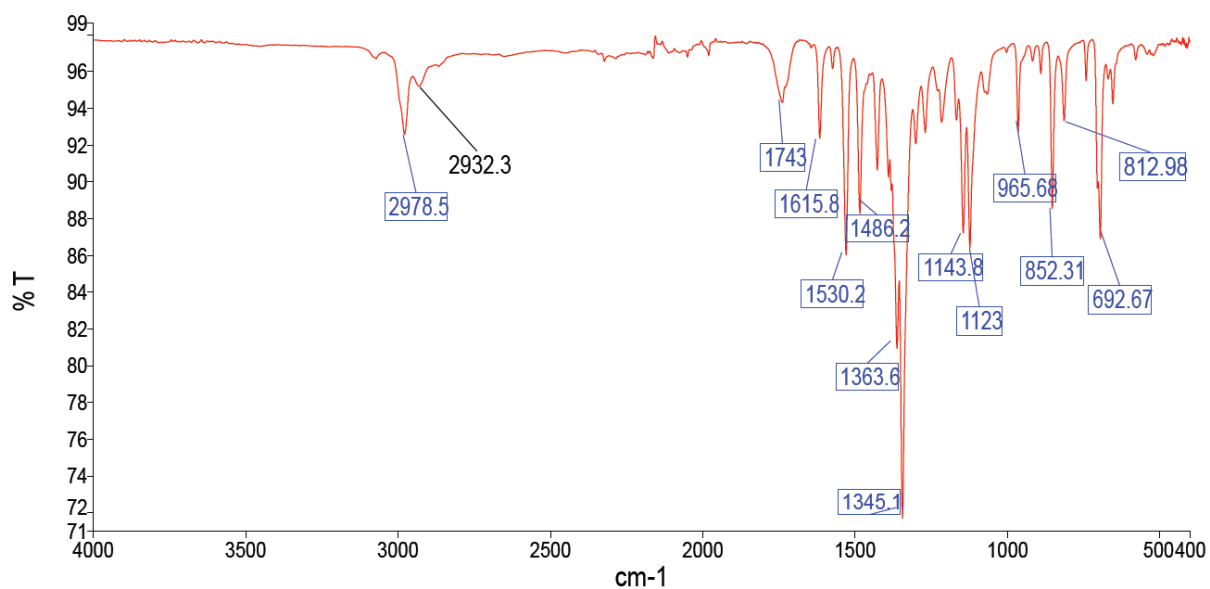


**Figure S13.** FTIR-ATR spectrum of isolated compound **2g**, synthesized by RAM.

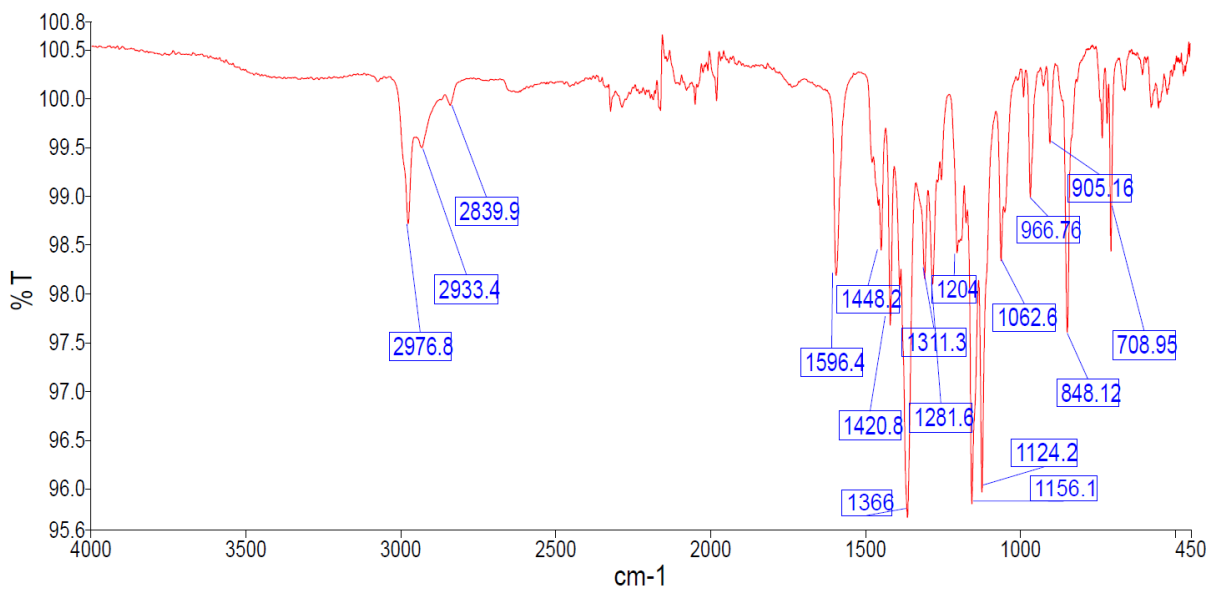


**Figure S14.** FTIR-ATR spectrum of isolated compound **2h**, synthesized by RAM.

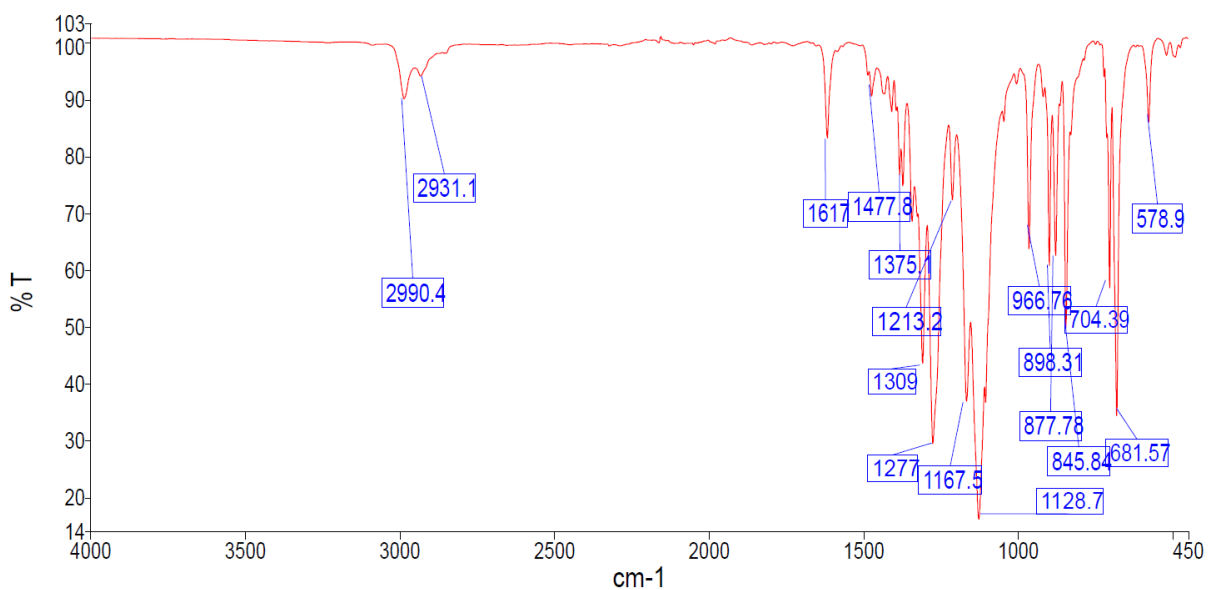


**Figure S15.** FTIR-ATR spectrum of isolated compound **2i**, synthesized by RAM.

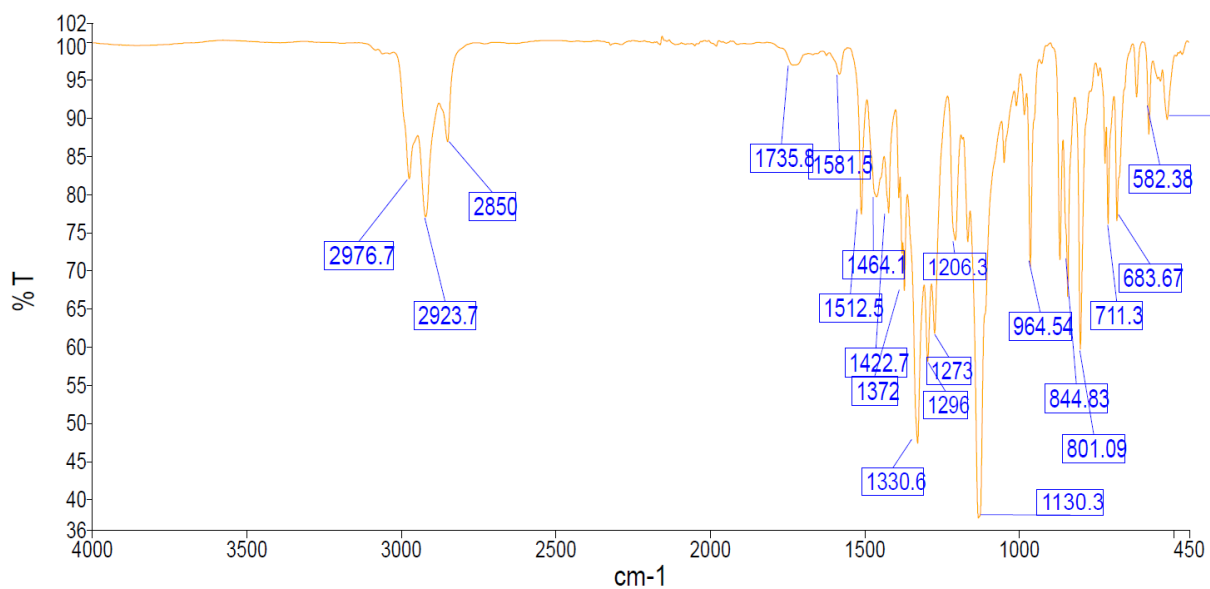


**Figure S16.** FTIR-ATR spectrum of isolated compound **2j**, synthesized by RAM.

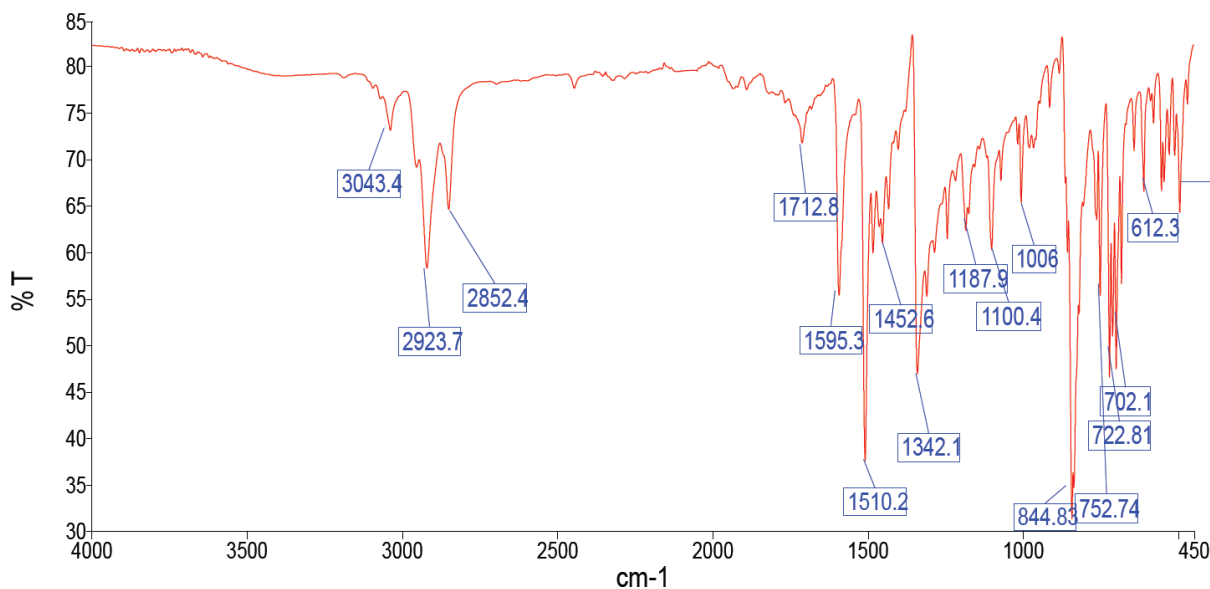


**Figure S17.** FTIR-ATR spectrum of isolated compound **3a/b**, synthesized by RAM.

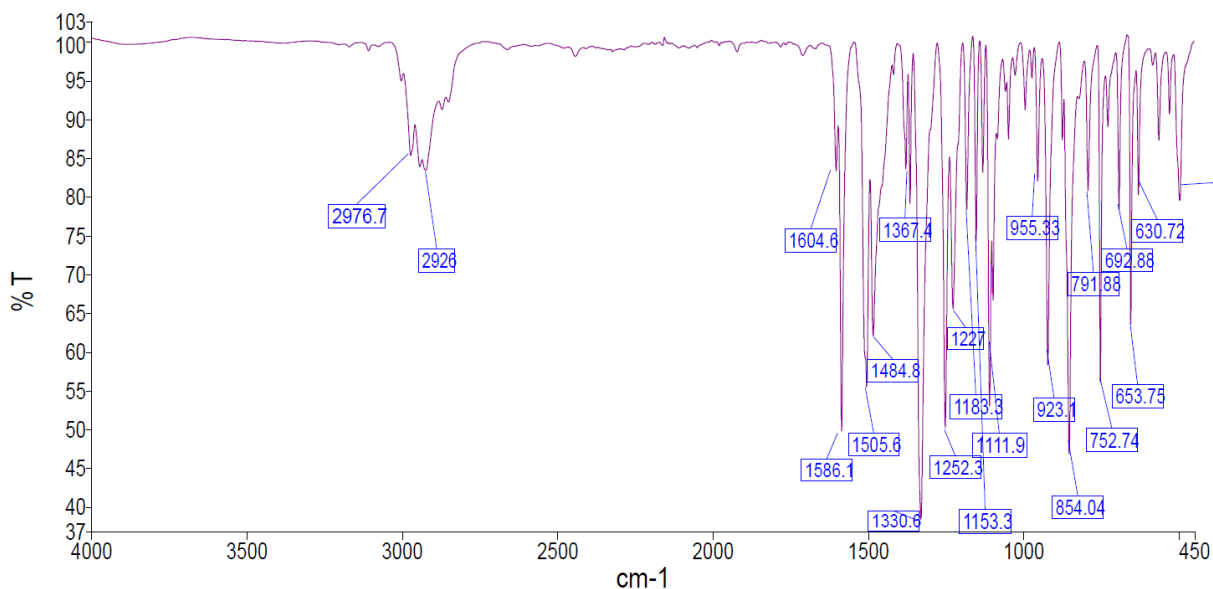


**Figure S18.** FTIR-ATR spectrum of isolated compound TEMPO-trapped intermediate, synthesized by RAM.

## 12. $^1\text{H}$ and $^{13}\text{C}$ NMR Data for Isolated Products 2a-2j and TEMPO-trapped intermediate

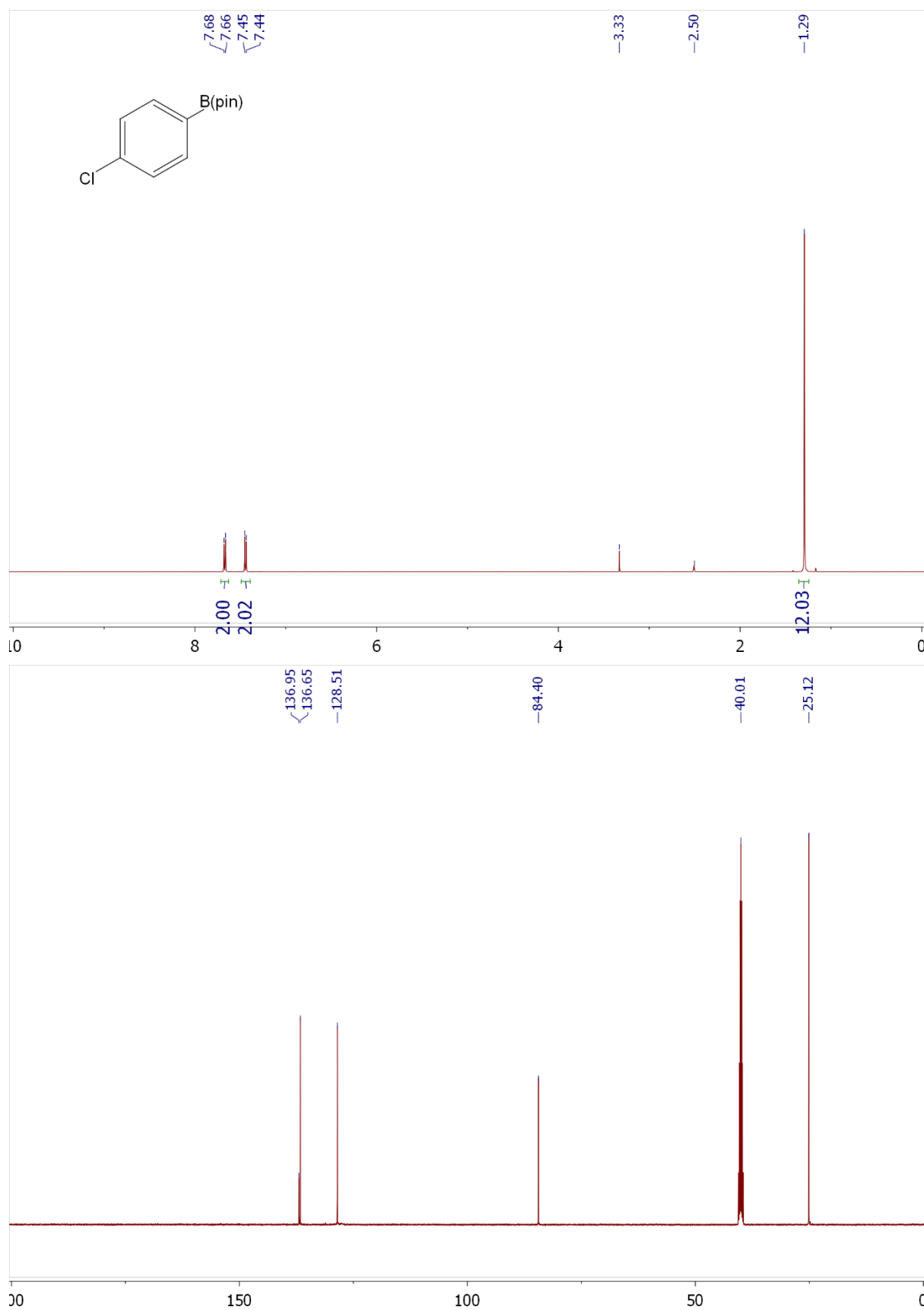


**Figure S19.**  $^1\text{H}$  (top) and  $^{13}\text{C}$  (bottom) NMR spectra for isolated compound **2a**, synthesized by RAM.

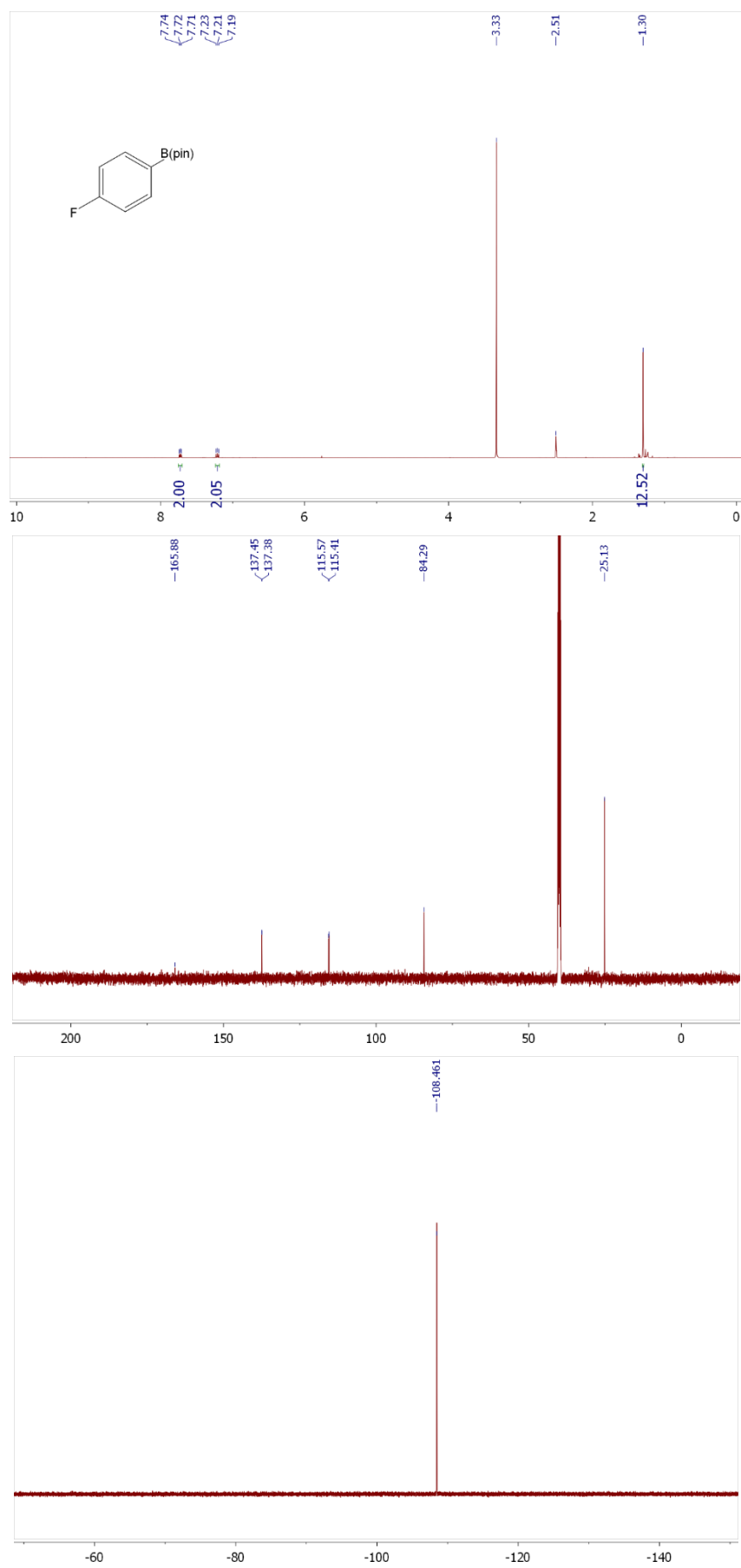


**Figure S20.**  $^1\text{H}$  (top),  $^{13}\text{C}$  (middle) and  $^{19}\text{F}$  (bottom) NMR spectra for isolated compound **2b**, synthesized by RAM.

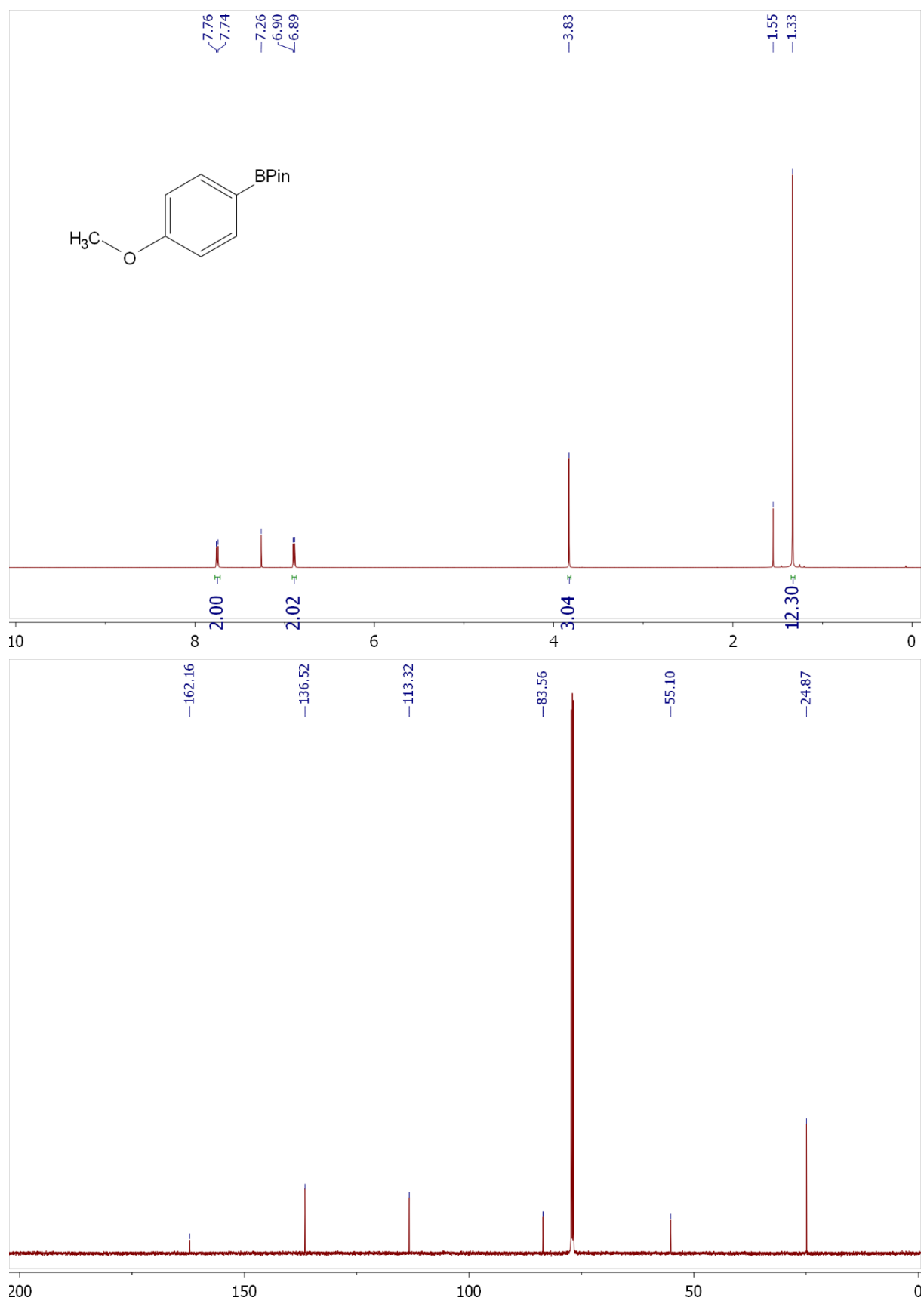


**Figure S21.**  $^1\text{H}$  (top) and  $^{13}\text{C}$  (bottom) NMR spectra for isolated compound **2c**, synthesized by RAM.

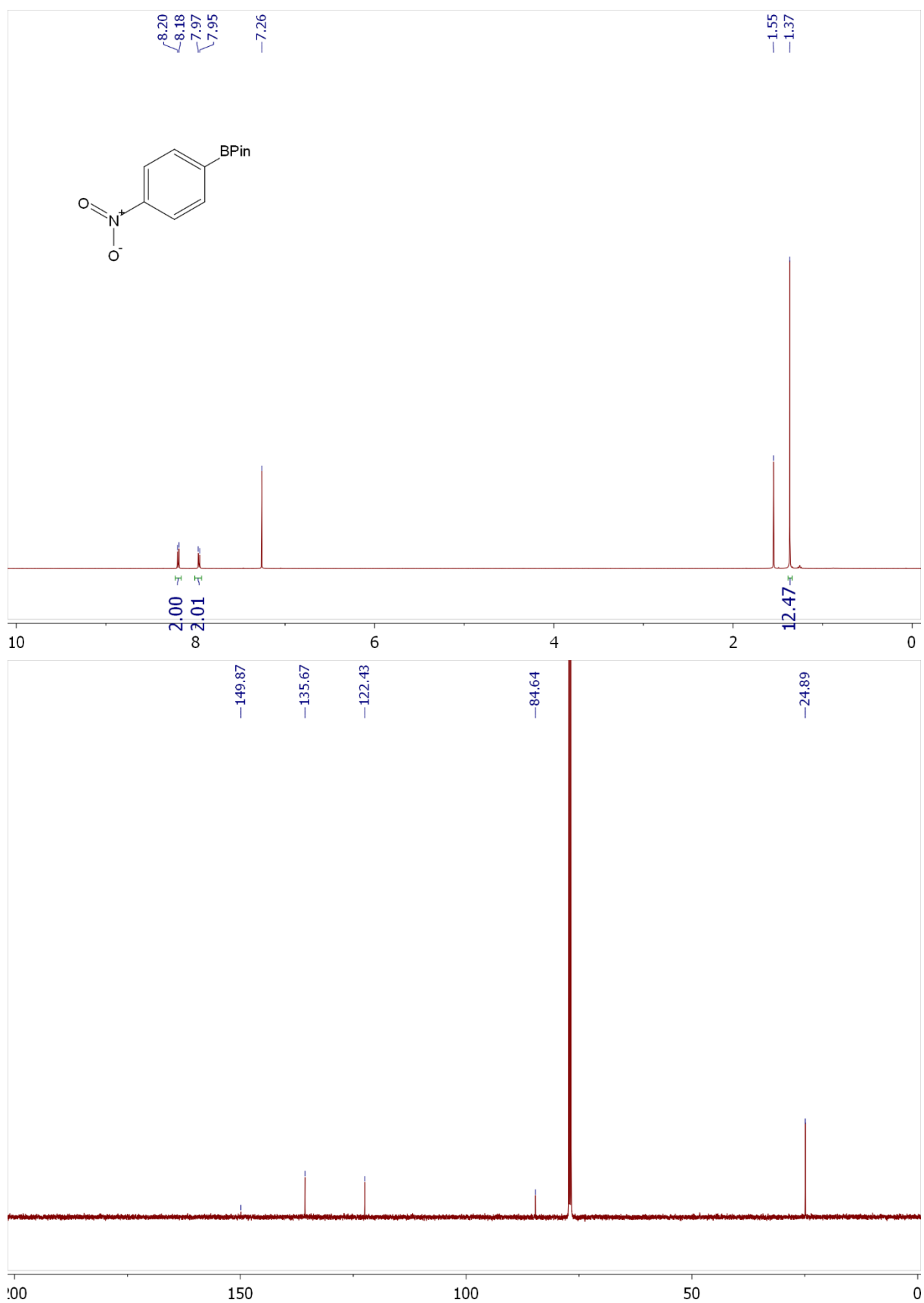


**Figure S22.**  $^1\text{H}$  (top) and  $^{13}\text{C}$  (bottom) NMR spectra for isolated compound **2d**, synthesized by RAM.

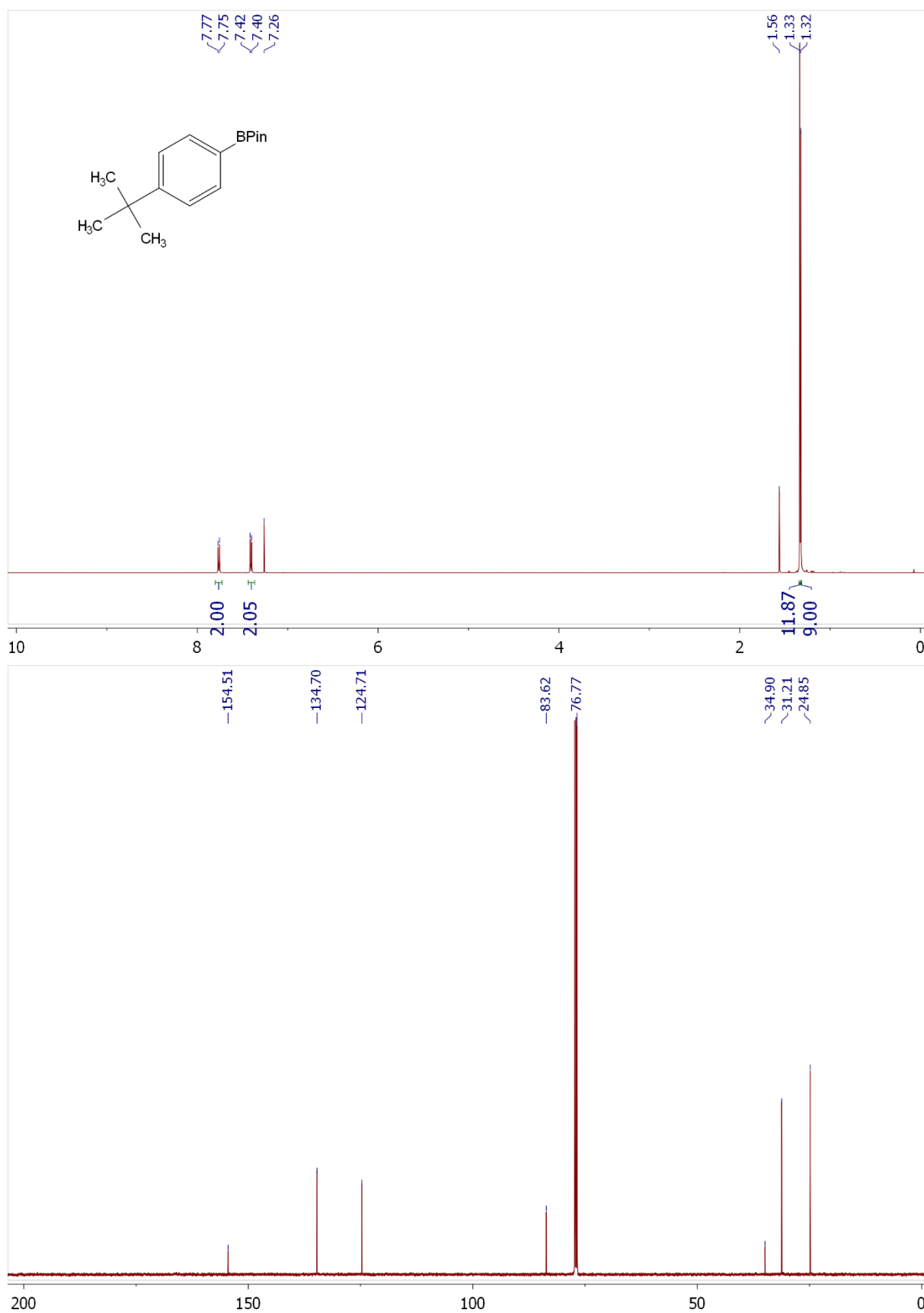


**Figure S23.**  $^1\text{H}$  (top) and  $^{13}\text{C}$  (bottom) NMR spectra for isolated compound **2e**, synthesized by RAM.

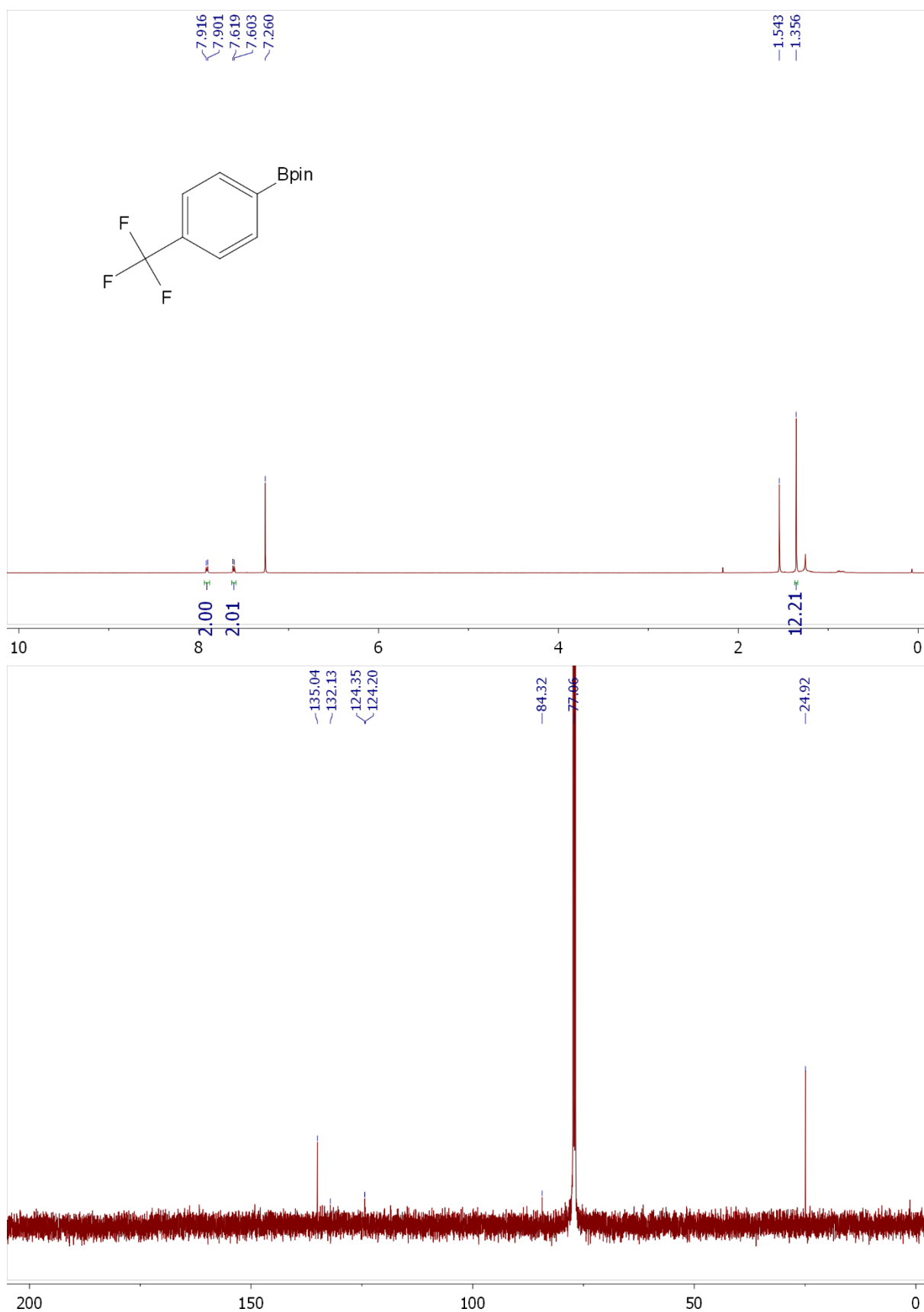


**Figure S24.** <sup>1</sup>H (top) and <sup>13</sup>C (bottom) NMR spectra for isolated compound **2f**, synthesized by RAM.

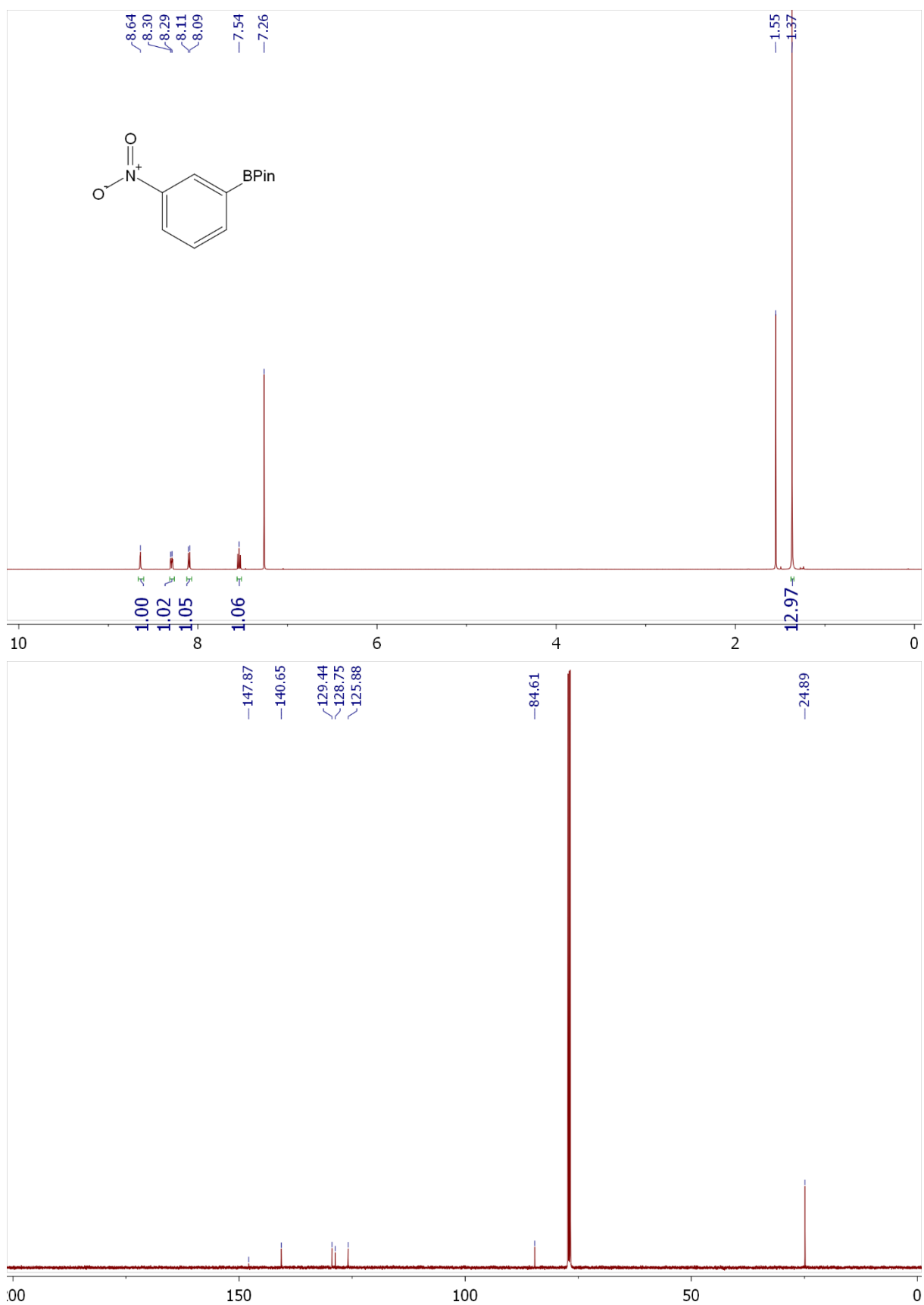


**Figure S25.** <sup>1</sup>H (top) and <sup>13</sup>C (bottom) NMR spectra for isolated compound **2g**, synthesized by RAM.

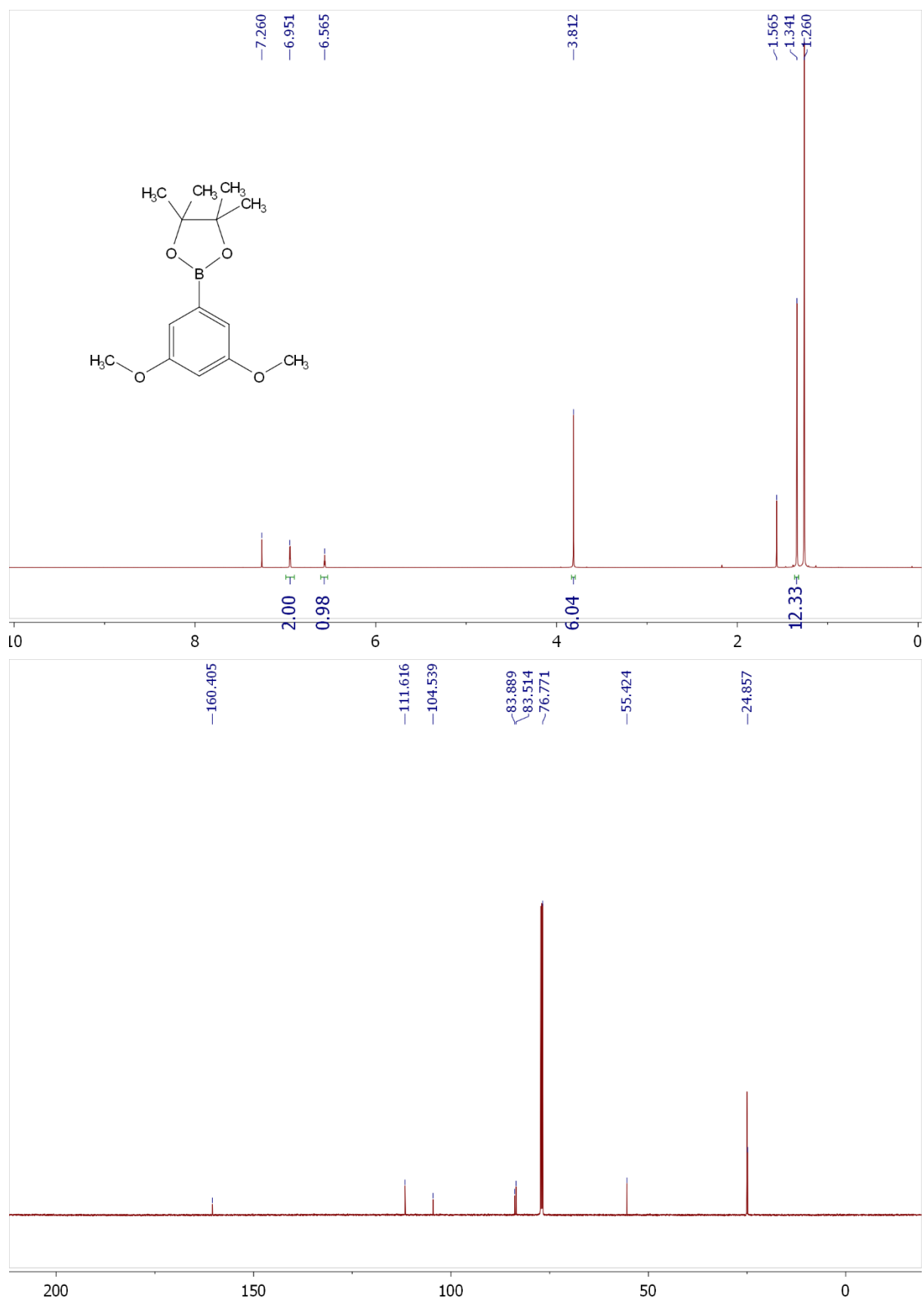


**Figure S26.** <sup>1</sup>H (top) and <sup>13</sup>C (bottom) NMR spectra for isolated compound **2h**, synthesized by RAM.

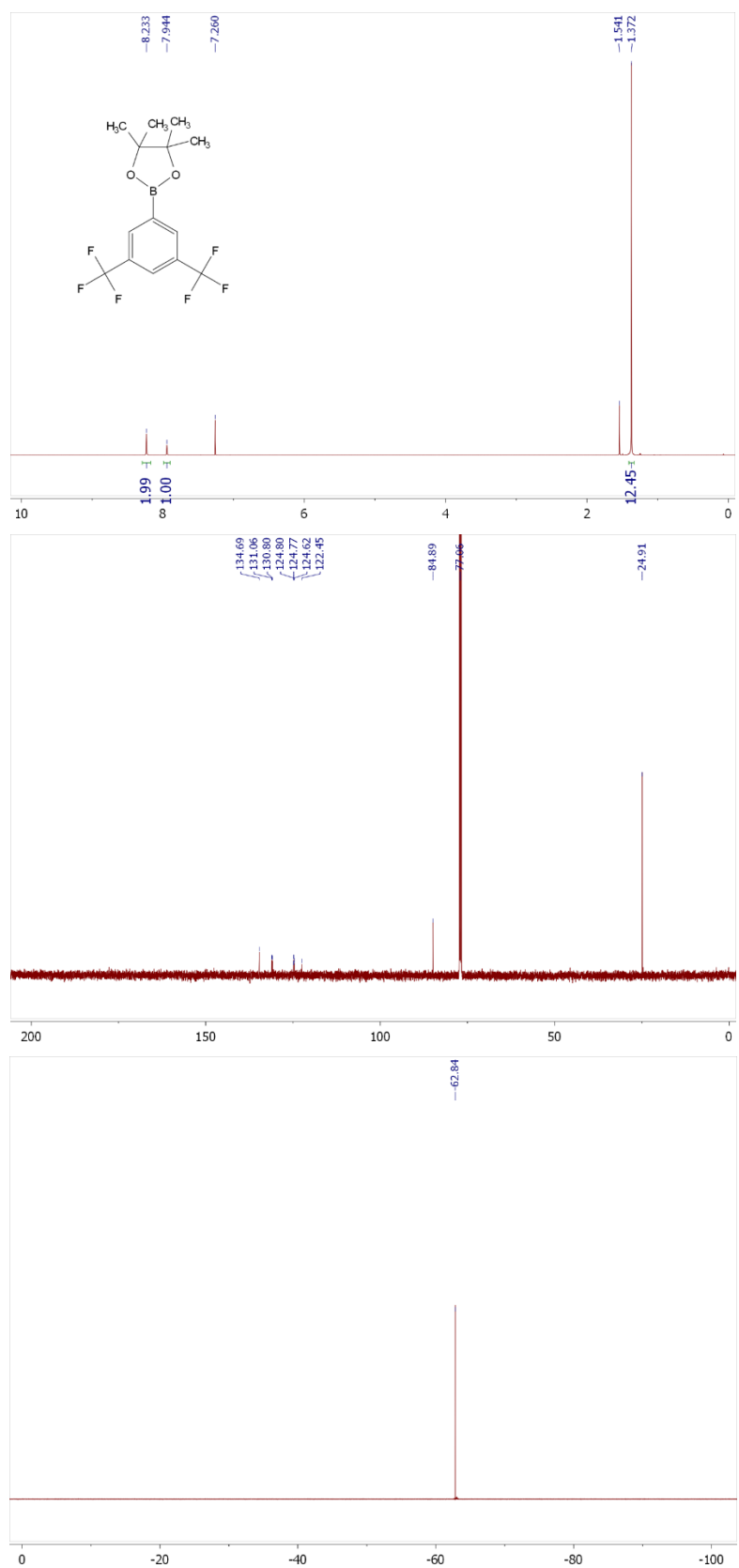


**Figure S27.** (top)  $^1\text{H}$ , (middle)  $^{13}\text{C}$  NMR and (bottom)  $^{19}\text{F}$  NMR spectra for isolated compound **2i**, synthesized by RAM.



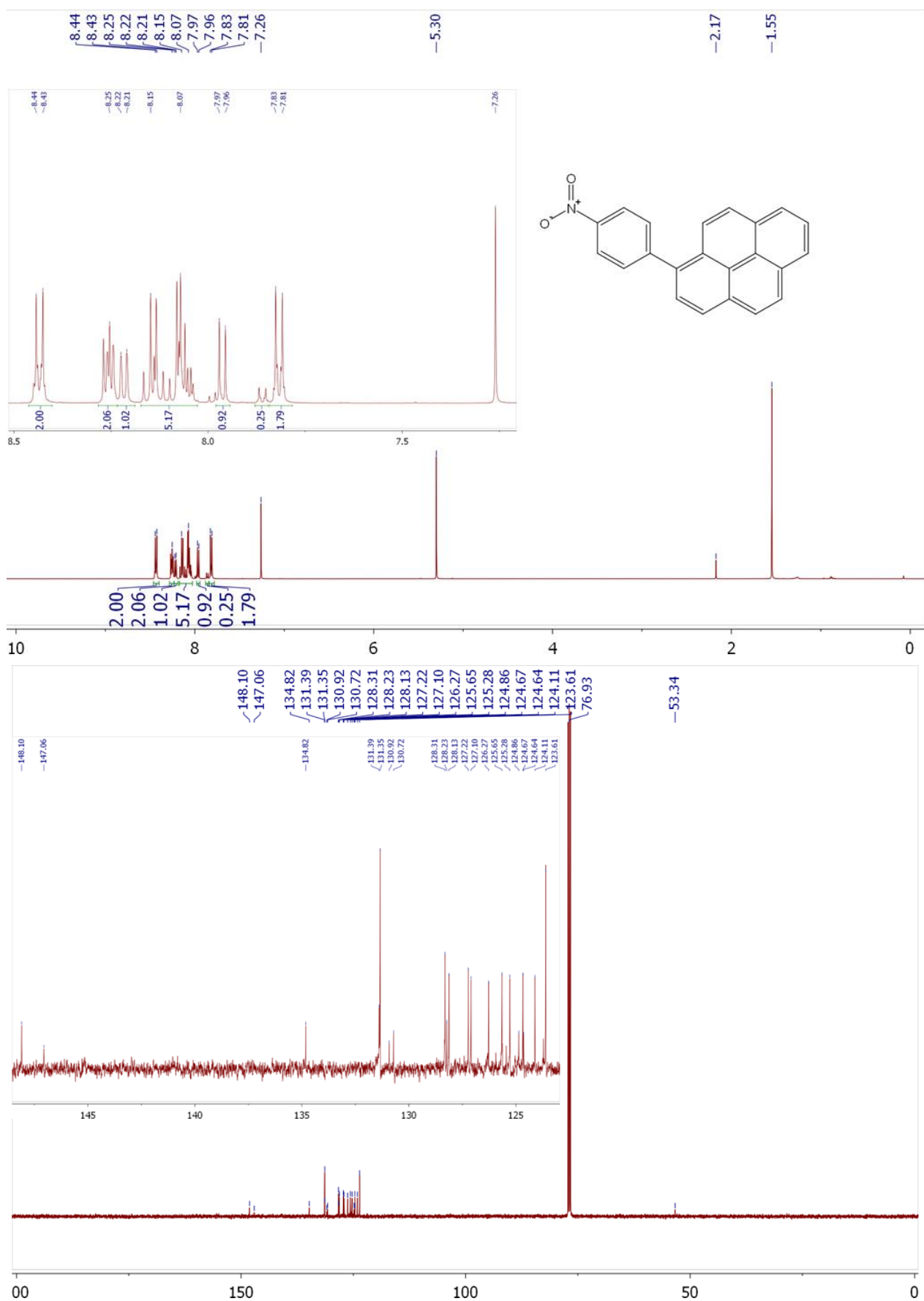


**Figure S29.** <sup>1</sup>H (top) and <sup>13</sup>C (bottom) NMR spectra for isolated compound **3a/3b**, synthesized by RAM.

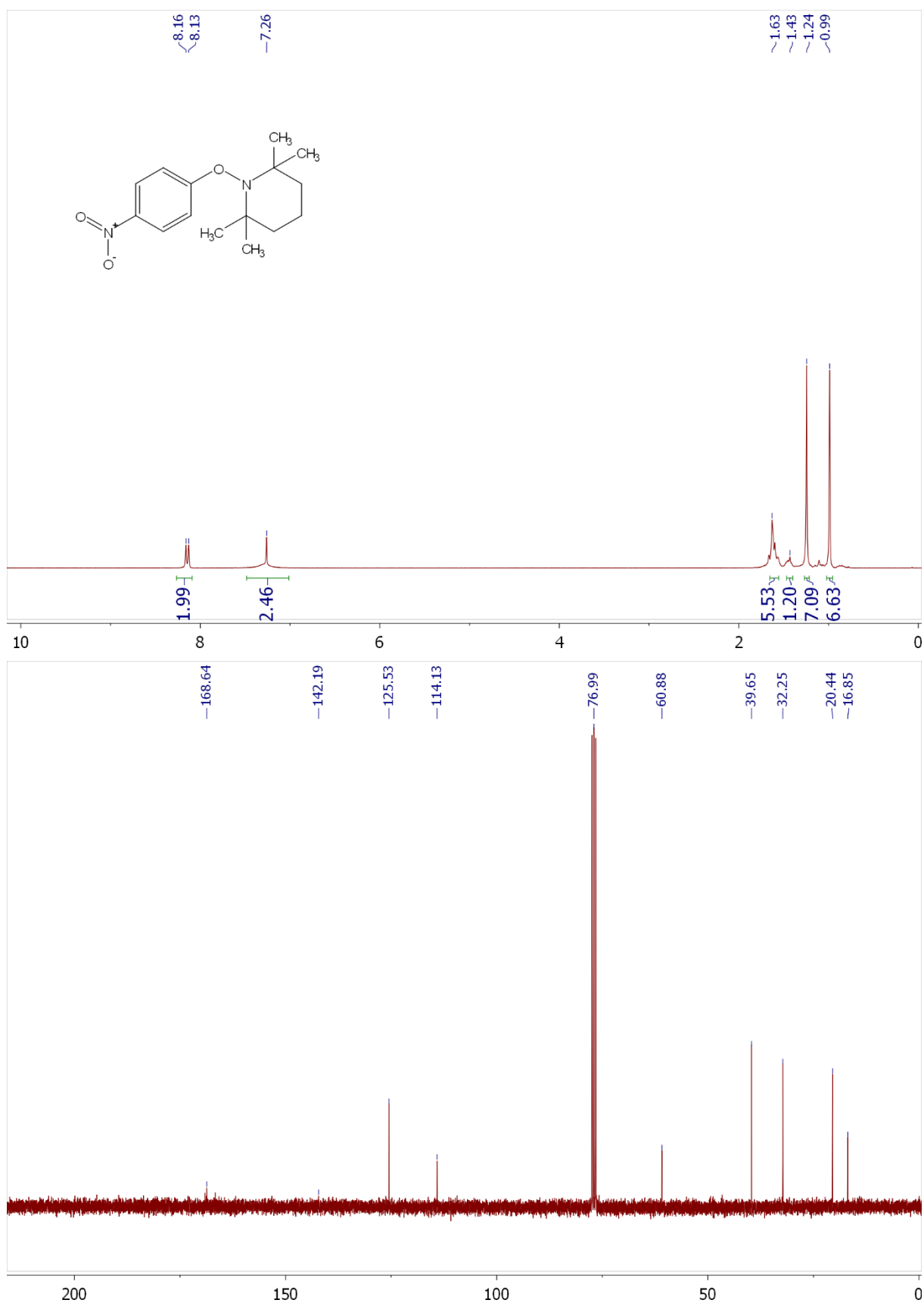


**Figure S30.** (top)  $^1\text{H}$  and (bottom)  $^{13}\text{C}$  NMR spectra for isolated TEMPO-trapped intermediate.

### 13. References

- [1] R. Cai, M. Lu, E. Y. Aguilera, Y. Xi, N. G. Akhmedov, J. L. Petersen, H. Chen and X. Shi, *Angew. Chem. Int. Ed.* 2015, **54**, 8772.
- [2] J. D. Firth and I. J. S. Fairlamb, *Org. Lett.* 2020, **22**, 7057.
- [3] B. Wrackmeyer, *Prog. Nucl. Magn. Reson. Spectrosc.* 1979, **12**, 227.
- [4] N. F. Pelz, A. R. Woodward, H. E. Burks, J. D. Sieber and J. P. Morken, *J. Am. Chem. Soc.* 2004, **126**, 16328.